Dimethylacetamide Sorption Kinetics in a Urethane/Urea/Ether Block Copolymer

M. M. GOU,[1] W. J. KOROS,[1,*] and G. GOLDMAN[2]

[1]The University of Texas at Austin, The Department of Chemical Engineering, Austin, Texas 78712;
[2]E. I. DuPont de Nemours, Engineering Technology Laboratory, Wilmington, Delaware 19880

SYNOPSIS

Polymer solvent interactions in a block polyurethane/urea/ether polymer belonging to the spandex family are considered in this article. Independent analysis of the sorption isotherms for dimethylacetamide (DMAc) in the spandex polymer as a function of vapor activity and temperature were presented in a previous article. A second aspect in understanding solvent/polymer interactions is the kinetics of desorption. Characterization of the solvent devolatilization is an important aspect of the drying procedure to guide processing protocols to eliminate residual solvent in the final spandex products, especially for medical applications [E. Hicks, A. Ultee, and J. Drougas, *Science*, **147**, 373 (1965); J. W. Boretos and W. S. Pierce, *J. Biomed. Mater. Res.*, **2**, 121 (1968); P. M. Knight and D. J. Lyman, *J. Membr. Sci.*, **17**, 245 (1984)]. This article reports data for desorption kinetics under nominally isothermal conditions to provide diffusion coefficients as a function of polymer phase concentration and temperature. Desorption curves were found to be Fickian at least up to the half-time of desorption. Diffusion coefficients were therefore calculated using a half-time method. Temperature effects upon sorption or desorption were measured to obtain corrected diffusion coefficients and found to be significantly different than the apparent diffusion coefficient measured from a conventional McBain sorption cell.

INTRODUCTION

Spandex polymers are a versatile class of thermoplastic elastomers whose major application is in the textile industry. Spandex threads are formed by extrusion of a polymer–solvent solution through a spinneret with subsequent windup following devolatilization of the solvent. The present study of the kinetics of devolatilization was undertaken to determine diffusion coefficients as a function of polymer phase concentration and temperature. Two types of spandex were examined: one a "clear" solution and the other an opaque or "white" solution with approximately 2% of TiO_2 added as a whitening agent. The effect of the TiO_2 as a nucleating agent for hard-segment aggregation is also examined in a comparison of the two types of spandex solutions.

The diffusion coefficients were measured with two systems: One approach involved the use of a conventional McBain sorption cell, and the other was based on a new design involving a semi-infinite slab desorption analysis.[1] Due to the basic experimental setup, the McBain technique is subject more to nonisothermal effects due to evaporation and condensation heat loads. Comparison of the results from the two systems allows evaluation of the accuracy of simple methods for dealing with the effect of temperature increase or drop upon sorption or desorption on the diffusion coefficient.

EXPERIMENTAL

Materials

The spandex polymer used in this study is a segmented polyurethane consisting of a hard segment (a urea), melting above 200°C, and a soft segment

* To whom correspondence should be addressed.

Journal of Applied Polymer Science, Vol. 51, 1685–1699 (1994)
 CCC 0021-8995/94/101685-15

[a poly(ether glycol)], melting at approximately 50°C. Both segments are polymeric and connected by urethane linkages. The polymer forms a clear viscous solution in dimethylacetamide (DMAc). This type of spandex is transparent and is referred to as "clear." The presence of $\approx$ 2.0% TiO_2 as a whitening agent in some samples transforms it to a white opaque material that will be designated as "white." The white solutions are identical to the clear except for the addition of small amounts of TiO_2 pigment. The general structure of the spandex polymer is shown below[2]:

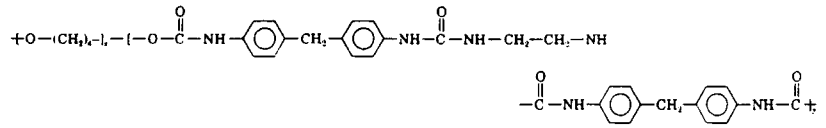

where x = 15–30 and y = 1–5.

Procedure

Kinetic measurements of desorption of DMAc in spandex were made using a conventional sorption cell, also used to obtain equilibrium sorption isotherms reported in an earlier article.[3] The kinetic measurements were done by placing a tared sample pan loaded with spandex solution in the chamber. To ensure no predrying of the sample, approximately 3–4 mL of pure DMAc was placed at the bottom of the chamber before inserting the sample. As with the isotherms, the system was carefully evacuated, avoiding bubbling and drying of the sample. The system was allowed to reach the saturated vapor pressure for the desired temperature by evaporation of the solvent in the chamber. If more solvent were needed, some could also be released from the supply ampule. The sample reached saturation when the weight was constant and no further uptake occurred. At this point, a timer was started simultaneously with opening the valve to vacuum to begin the integral desorption experiment. Readings of weight loss vs. time were used to plot the sorption curves and to obtain diffusion coefficients for the interaction pair.

THEORY AND BACKGROUND

The diffusion coefficient provides a quantitative measure of the rate at which a diffusion process occurs. It is defined in terms of Fick's first law, where **D** is the diffusion coefficient or the rate of transfer of the diffusing substance across the unit area of a section divided by the gradient of concentration at the section. This equation was developed for an isotropic medium; so by assuming that Fickian diffusion occurs only in the x-direction, performing a mass balance on an element volume yields Fick's second law:

$$\frac{\partial C}{\partial t} = \frac{\partial C}{\partial x}\left(\mathbf{D}\frac{\partial C}{\partial x}\right) \tag{1}$$

where t is time; C, concentration; and **D**, the diffusion coefficient. This expression neglects the frame of reference term due to convection, and in all subsequent derivations, this term will also be neglected since it will not be taken into consideration in this study.

In some cases, especially those of diffusion in dilute solutions, **D** can be taken as reasonably constant, whereas at high polymer concentrations, **D** may depend heavily on concentration. Crank[4] suggested a conventional method to determine the quantitative dependence of the diffusion coefficient on local concentration, using the half-times of sorption experiments carried out for a number of different penetrant pressures. This method, detailed by Crank and Park,[5] depends on the fact that a mean value $\mathbf{D}_{AV}$ provides a reasonable approximation of the variable diffusion coefficient averaged over the entire range of concentration of the experiment. When **D** varies moderately with C, this integral value of **D** can be used following the relation

$$\mathbf{D}_{AV} = \frac{1}{C_f}\int_0^{C_f} \mathbf{D}\, dC \tag{2}$$

where 0 to C_f is the concentration range existing in the polymer during an experiment.

Fick's second law [eq. (1)] can be used to derive expressions to calculate **D**, as shown below. Although a constant **D** is assumed in deriving these equations, it is implied that for a concentration-dependent diffusion coefficient, as is the case of a polymer solution, the value of **D** obtained by these equations will be that of $\mathbf{D}_{AV}$ given by eq. (2).

The diffusion coefficient can be deduced by the sorption/desorption method in which the value of **D** is determined from the normalized rate of sorption or desorption. The equation is based on the assumptions that the concentration in the sheet is initially uniform and the surface concentrations are instantaneously brought to equilibrium with the external bath activity. The solution to Fick's second law can be written as

$$\frac{M_t}{M_\infty} = 1 - \frac{8}{\pi^2}\sum_{m=0}^{\infty}\frac{1}{(2m+1)^2} \times \exp\left[\frac{-\mathbf{D}(2m+1)^2\pi^2 t}{\mathbf{l}^2}\right] \quad (3)$$

where M_t is the amount of vapor absorbed by the polymer at time t in sorption experiments or desorbed in desorption experiments; M_∞, the equilibrium amount of sorption or desorption attained theoretically at infinite time; and **l**, the thickness of the polymer sample. For values of $M_t/M_\infty > 0.6$, eq. (3) can be reduced to

$$\frac{M_t}{M_\infty} = 1 - \frac{8}{\pi^2}\exp\left(\frac{-\mathbf{D}\pi^2 t}{\mathbf{l}^2}\right) \quad (4)$$

since at long times, terms beyond $m = 0$ are insignificant. By substituting the value of 0.5 for M_t/M_∞, the following relationship results:

$$\mathbf{D} = \frac{0.049\mathbf{l}^2}{t_{1/2}} \quad (5)$$

where $t_{1/2}$ corresponds to the time at which $M_t/M_\infty = 0.5$. Therefore, by measuring the half-time, the diffusion coefficient can be determined for a known sample thickness, if Fickian transport occurs. Similarly, an expression for the diffusion coefficient can be deduced by the use of initial rates of sorption and desorption. This method will yield an average diffusion coefficient from the initial sorption curve when plotted against the square root of time. Again, from Fick's second law [eq. (1)], the following equation can be derived, with the aid of Laplace transforms:

$$\frac{M_t}{M_\infty} = 4\left(\frac{\mathbf{D}t}{\mathbf{l}^2}\right)^{1/2} \times \left[\frac{1}{\sqrt{\pi}} + 2\sum_{m=0}^{\infty}(-1)^m \text{ierfc}\frac{m\mathbf{l}}{\sqrt{(\mathbf{D}t)}}\right] \quad (6)$$

For values of $M_t/M_\infty < 0.6$, eq. (6) may be approximated by

$$\frac{M_t}{M_\infty} = 4\left(\frac{\mathbf{D}t}{\pi\mathbf{l}^2}\right)^{1/2} \quad (7)$$

If the early time sorption curve in an experiment in which **D** is concentration-dependent is observed, the average diffusion coefficient $\mathbf{D}_{AV}$ can be obtained from eq. (7), which is an approximation corresponding to eq. (2). If a sorption curve plotted vs. $\sqrt{t}/\mathbf{l}$ is found to be linear as least as far as $M_t/M_\infty < 0.6$, then eqs. (7) and (5) will yield the same diffusion coefficient since eq. (7) can be reduced to the same form as eq. (5).

The diffusion coefficient can take on various complex forms as a function of local concentration. Basic characteristics of sorption and desorption for Fickian processes have been summarized by Fujita et al.[6-8] Some of these important Fickian characteristics are outlined below for future reference:

(a) For both sorption and desorption curves, plots of M_t/M_∞ plotted vs. $\sqrt{t}$ are linear up to 0.6. If $\mathbf{D}(C)$ is an increasing function of C, the sorption curve is linear even beyond $M_t/M_\infty = 0.6$.

(b) Above the linear portions, both sorption and desorption curves become concave toward the abscissa and approach the final equilibrium value gradually.

(c) If the initial concentration, C_i, and the final concentration, C_f, are held fixed, a series of sorption curves for films of different thicknesses are superimposable on a single curve when M_t/M_∞ is plotted in the form of a reduced curve, i.e., M_t vs. $\sqrt{t}/\mathbf{l}$.

(d) The reduced sorption curve always lies above the corresponding reduced desorption curve if **D** is an increasing function of C in the region between C_i and C_f. If **D** passes through a maximum at a certain concentration between the given C_i and C_f, the two curves may intersect at a point.

Criteria (a)-(c) are independent of the form of **D** as a function of C. The fulfillment of these three criteria determines whether an experimental isothermal system exhibits Fickian transport behavior.

In noncrystalline, rubbery polymers, especially during desorption, diffusion is generally Fickian because the chain segments respond rapidly to changes

in their condition. Even though the mechanical properties of soft/hard block copolymers such as styrene–butadiene–styrene (SBS) copolymers and segmented polyurethanes are like those of simple elastomers, the sorption/desorption kinetics of such materials often deviate from at least one of the Fickian criteria. Odani et al.[8] reported that the sorption/desorption behavior of *n*-hexane vapor in SBS block copolymers of different film thicknesses did not obey Fickian criterion (c), although the individual sorption/desorption curves curves obeyed Fickian criteria (a) and (b). On the other hand, they showed that sorption/desorption processes in homopolybutadiene films were purely Fickian. Chiang and Sefton showed similar sample thickness dependence of sorption/desorption kinetics of cyclohexane in SBS and reported the effect of internal stress of samples also by comparing the sorbent transport kinetics of various samples prepared by different casting methods.[9]

All the anomalous sorption/desorption phenomena described above were generally explained by the interaction between the heterogeneous segment domains. Whereas the chemical structure of spandex is quite different from SB or SBS copolymers, there are some common features: SBS copolymers have hard/soft microdomains with hard segments whose T_g is far above the use temperature and soft segments whose T_g is far below the use temperature. Spandex also has hard and soft segments, but the hard segments are believed to be crystalline and less easily penetrable.

Temperature Effects During Sorption or Desorption

The effect of the heat of sorption on vapor sorption kinetic results was studied by Armstrong and Stannett.[10,11] The influence of heating effects on the diffusion coefficient were treated for water-vapor diffusion into wool fibers and ethyl cellulose films. Temperature increases in the samples caused large decreases in the apparent diffusion constant obtained by usual half-time experiments. A mathematical model was developed to correct the rates of sorption and desorption for these heat effects. The model was derived from standard differential equations governing heat and mass transfer after applying some simplifying assumptions. The solution was obtained for a film assuming unidirectional diffusion in a film of constant thickness "2b" where the film surfaces are in equilibrium at all times with the external vapor of constant temperature throughout the experiment. The corrections increase progressively with increasing concentration and temperature. The model corrects for heat gained during sorption that heats the sample, creating a new effective sample temperature higher than that of the surroundings. This new temperature would make the sample sorb faster than it should for that temperature and vice versa; for desorption, the sample cools as it desorbs and desorbs at a lower rate for a specific nominal temperature. Because of the much lower heat of vaporization of organic solvents compared to that of water, such temperature effects are generally not considered for studies involving organic penetrants. Recently, however, temperature effects were reported by Waksman et al. to be important for a toluene/natural rubber system.[12] The heat of vaporization of DMAc is also similar to that of water, and, hence, heat effects were suspected to be of possible importance in our work.

The sample specific heat capacity was assumed to be independent of the "undesorbed fraction," defined as $\{1 - M_t/M_\infty\}$, and a linear relationship was assumed between the undesorbed fraction and the uniform internal temperature of the sample, due to the more rapid nature of heat vs. mass transfer. The solution to the heat and mass balance gave an expression for the diffusion coefficient, **D**, from a limiting slope of the undesorbed fraction plotted as a function of time on a semilogarithmic scale. The value of **D** is thus determined from the following expression:

$$\mathbf{D} = \frac{-1}{\lambda^2}\left[\frac{d \ln\left[1 - \frac{M_t}{M_\infty}\right]}{dt}\right] = \frac{-1}{\lambda^2}(\text{slope}) \qquad (8)$$

where λ is the first eigenvalue of the equation

$$\frac{1}{L\omega}\left[\frac{H}{b\rho(\text{slope})} - C_p\right] = \frac{\tan(\lambda b)}{\lambda b} \qquad (9)$$

which is a simplified expression of the model solution.

In this expression, L is the isosteric heat of sorption of the vapor; ω, the "temperature coefficient of regain"; H, the heat-transfer coefficient between the sample and the surroundings; b, the half-thickness of the sample; ρ, the density of the sample; and C_p, the specific heat capacity of the sample. The heat-transfer coefficient may be calculated from a radiation heat balance using the Stefan–Boltzmann constant, σ, as shown in the Appendix:

$$H = \sigma(T_0 + T_{\text{inc}})(T_0^2 + T_{\text{inc}}^2) \qquad (10)$$

where T_0 is the temperature of the surroundings and $T_{inc} = T_0 + \Delta T$ is the incremental temperature of the sample, where ΔT is the temperature change of the sample during sorption or desorption. The temperature drop during desorption may be measured experimentally or estimated from a wet and dry bulb analysis as described in Bird et al.[13] To determine the temperature coefficient of regain, ω, and the heat of sorption, L, equilibrium sorption isotherms are needed to obtain graphs of constant concentration or isosteres.[10] These isostere graphs are plots of the DMAc partial pressure at each concentration vs. the vapor pressure corresponding to the initial temperature of the sample prior to desorption as shown in Figure 1(A). The slope of these lines times the heat of vaporization of the vapor allows determination of the isosteric heat of sorption, L. These plots also yield ω by a series of manipulations described by Armstrong and Stannett as described below.

From the isostere lines, values of the corresponding saturation vapor pressure (p_0) are read for each concentration at a specific partial pressures. From this vapor pressure, a temperature, T, can be determined, which is then plotted as an "undesorbed fraction" graph, as $\ln\{1 - M_t/M_\infty\}$ vs. $(T - T_0)$, where T_0 is the temperature of the experiment or surroundings as shown in Figure 1(B). The value of ω is then determined from the initial slope of the uptake lines in units of (1/°C). At this point, the parameters composing the left-hand side of eq. (9) are determined, and a value of λ can be found by solving first for λb as shown in Figure 2.

Once the value of λ is obtained, a value for the diffusion coefficient can be calculated from eq. (8). A qualitative measure of whether a correction for temperature effects on diffusion is needed can be obtained from a dimensionless number χ, defined

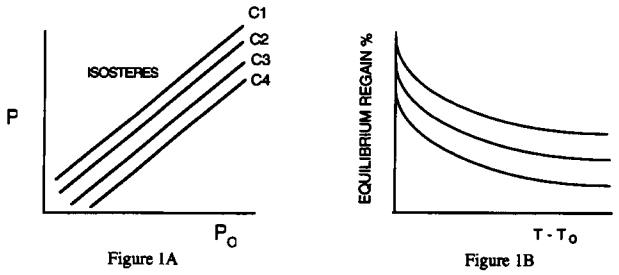

Figure 1A Figure 1B

Figure 1 (A) Sketch of isostere graphs of partial pressure vs. vapor pressure. (B) Sketch of the equilibrium regain or undesorbed fraction vs. temperature difference $(T - T_0)$ from which values of ω are calculated. Both plots are necessary in obtaining temperature-correction parameters.

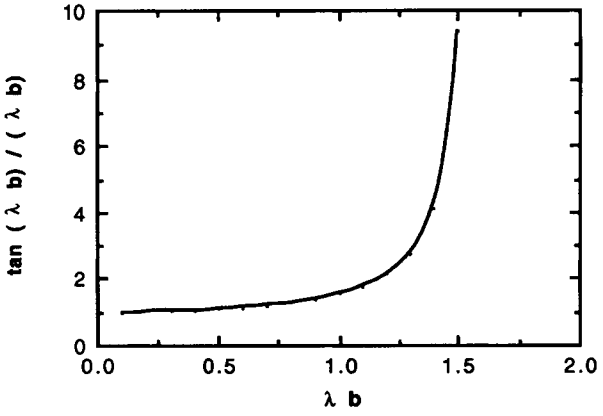

Figure 2 Plot of solution of the temperature correction eq. (9). The right-hand side of the equation vs. λb is plotted to solve for λb given the value of the left-hand side of the equation.

by eq. (11):

$$\chi = \frac{Hb}{L\omega\rho\mathbf{D}_{measured}} \tag{11}$$

If χ is small ($\chi < 1.0$), the process is heat-transfer-controlled and the diffusion coefficient estimate requires corrections, whereas if χ is large ($\chi > 10$), the process is diffusion-rate-controlled and needs no corrections. From this dimensionless number, the magnitude of the corrections between the two extremes of λ were tabulated by Armstrong and Stannett for diffusion constants in films. A graph of the relation between χ and % correction for films is shown in Figure 3, where the % correction is defined as the fraction $[(\mathbf{D}_{corrected} - \mathbf{D}_{measured})/\mathbf{D}_{measured}] \times 100$, where $\mathbf{D}_{measured}$ is the uncorrected value.

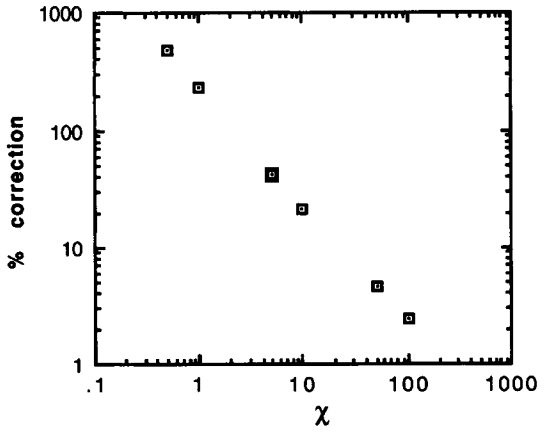

Figure 3 Graph of percent correction vs. χ where a log–log relationship is obtained. The relation obtained from this plot is shown in eq. (12).

The approximate empirical correlation obtained from the graph in Figure 3 to relate χ to percent correction is

$$\% \text{ correction} = 240 \frac{1}{\chi} \qquad (12)$$

RESULTS AND DISCUSSION

Desorption kinetic measurements, represented as M_t/M_∞ vs. $\sqrt{t}/l$ in Figure 4, are the results of a study performed to determine the effect of predrying on a sample. Although in the case of isothermal sorption equilibria there was no detectable difference between predrying or using an as-received sample (1), a study was done to compare the effect of these conditions on desorption kinetics. Figure 4(A) compares clear and white spandex for as-received samples. The insert is an expansion of the initial time desorption for closer scrutiny. A faster rate of

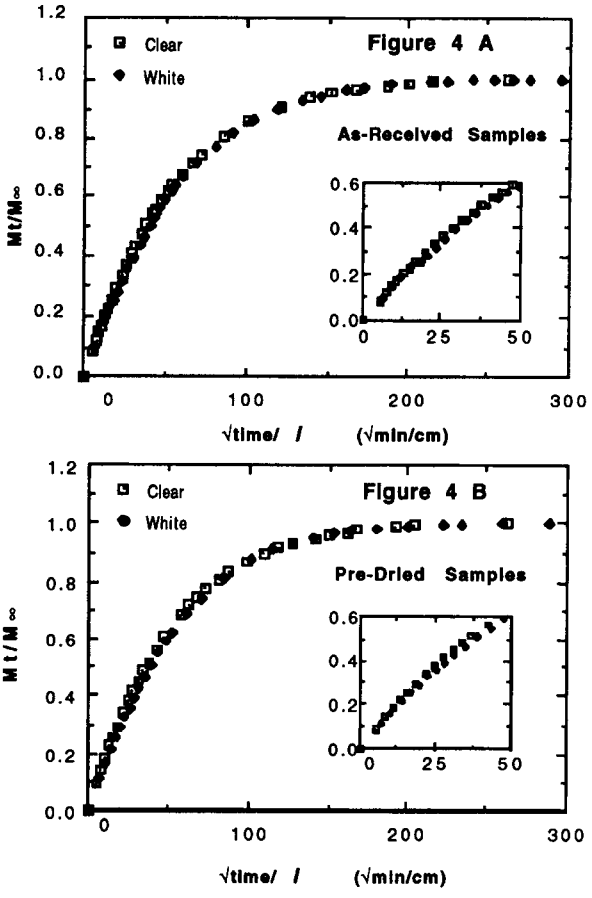

Figure 4 Comparison of kinetics of desorption between clear and white spandex in as-received and predried samples at 60°C.

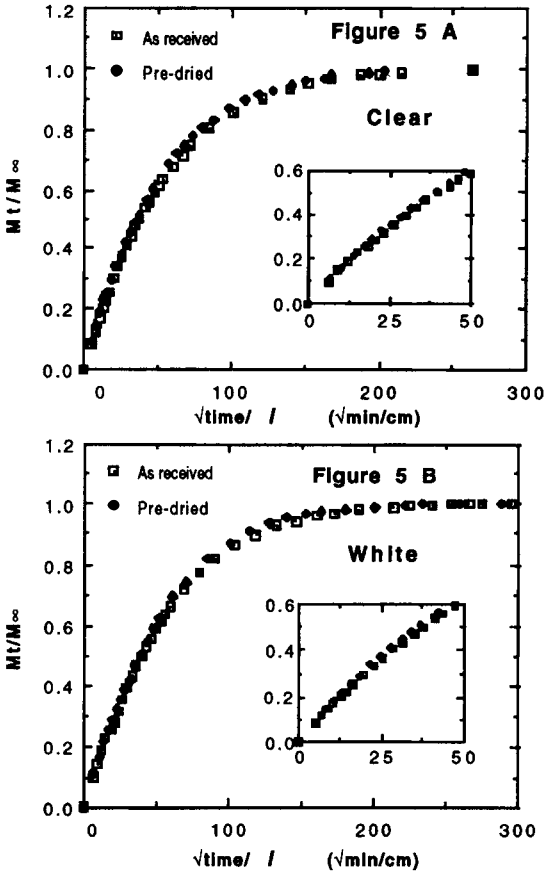

Figure 5 Comparison of kinetics of desorption between as-received and predried samples for both clear and white spandex.

desorption is observed for the clear vs. the white. Figure 4(B) indicates the same type of response for clear and white, where the clear, again, has a faster desorption rate even though the samples were predried. In comparing the clear and white rates, for both predried and undried samples, the clear material desorbed faster than did the white samples.

A similar comparison is made in Figure 5 by plotting the data from Figure 4 for the as-received clear sample vs. a predried clear sample in Figure 5(A) and the as-received white sample vs. a predried sample in Figure 5(B). Again, the inserts are expansions of the initial stage of desorption, and although the effect is not very large, the predried samples are slightly more rapid in desorbing than are the as-received for both clear and white types. No difference between the two was expected since the cross-linking does not appear to be affected as seen by the sorption isotherms. Possibly partially irreversible aggregation of hard segments occurs when the sample is dried totally, causing it to desorb faster

after resaturation even though given enough time to equilibrate the sorption level would become the same for each intermediate activity level. Fresh samples were used in all subsequent studies to avoid the possibility of any extraneous effects.

Integral desorption kinetics of DMAc from both types of spandex were performed at various temperatures ranging from 40 to 100°C. The data plotted in reduced form are shown in Figure 6. The curves are very reproducible; several runs were done at the same conditions and the shape of the curves were indistinguishable. The thickness, **l**, used in the abscissa of the plots was calculated from the known weight at each time t, since the area of the bottom of the pan is fixed and the density of the solutions were assumed to be constant to obtain a decreasing thickness with time. Since the densities of DMAc and the spandex were very similar (0.943 g/cc vs. 1, respectively), this was a satisfactory approximation.[14] As expected, the graphs show larger diffusion coefficients at higher temperatures for both clear and white spandex as indicated by the increasing slopes.

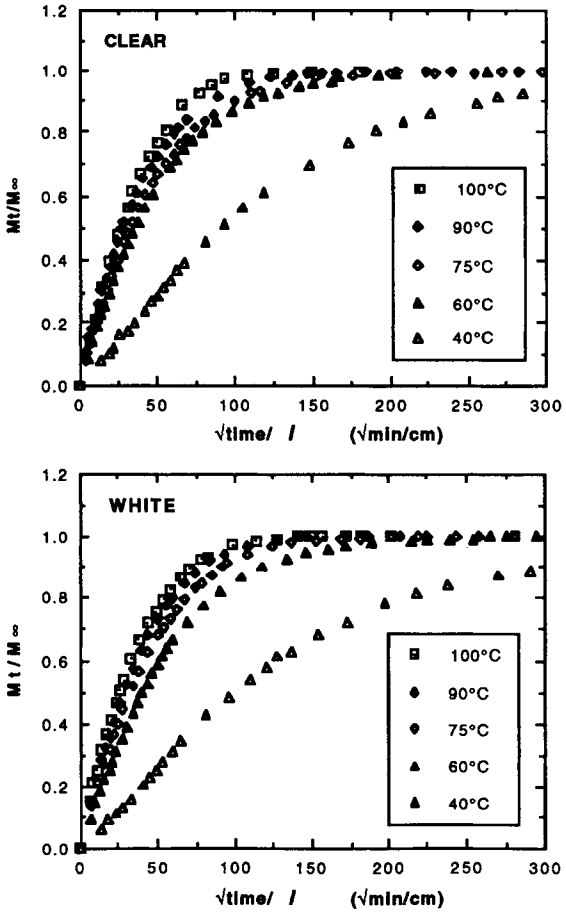

Figure 6 Desorption kinetics plot of fractional weight loss vs. $\sqrt{t}/l$ as reduced Fickian plots from which diffusion coefficients are calculated. Results are shown for clear and white spandex at temperatures from 40 to 100°C.

The thermally induced motions of small diffusate molecules such as gases are rapid compared to those of the polymer chain, especially at lower temperatures. Thus, the rate of diffusion is controlled mostly by the chain segmental movements. Diffusion takes place as a result of random Brownian jumps of the diffusate molecules within spaces between polymer chains. For very small penetrant molecules such as hydrogen, in most polymers, diffusion is postulated to occur with only a few chain segments being involved in the diffusion jumps, characterized by (a) dilute sorption behavior showing negligible departures from Henry's law of solubility, (b) concentration-independent diffusion coefficients, and (c) an apparent activation energy independent of temperature and concentration.[15] Diffusion of larger organic molecules, on the other hand, often involves (a) nondilute mixtures, solubility being a nonlinear function of concentration, (b) markedly concentration-dependent diffusion coefficients, and (c) temperature-dependent energies of activation for diffusion. Semilog plots of ln **D** vs. $1/T$ exhibit a significant convex downward curvature, as shown in Figure 7. It has been suggested[16] that the relationship between the average free volume, V_f, in a polymer–penetrant system and the minimum void volume, for diffusion of a penetrant is crucial to the type of behavior observed in polymer systems that are well above T_g. For very large penetrant molecules, this minimum void volume is much greater than V_f, so a large number of polymer segments must cooperate in any diffusive motion since the preexisting voids are not large enough for a void diffusion mechanism. This is the situation in which the polymer segmental mobility controls the diffusion.

The data for the curves in Figure 6 were plotted vs. theoretical Fickian curves obtained from half-time diffusion coefficients. This graph is included in the Appendix as Figure A.1. There is an almost ideal Fickian response in all curves for weight fractions up to about 0.6, which makes it acceptable to use the half-time method to calculate the diffusion coefficient. The long time curves show a slower response than that predicted by the long-term Fickian desorption. Previous work by Berens and Hopfenberg[17] on organic vapor sorption into monodisperse glassy polymer powders and others mentioned in their article show a similar response after a half-time Fickian response. Hopfenberg and Frisch, in an earlier article,[18] suggested that behavior ranging from ideal

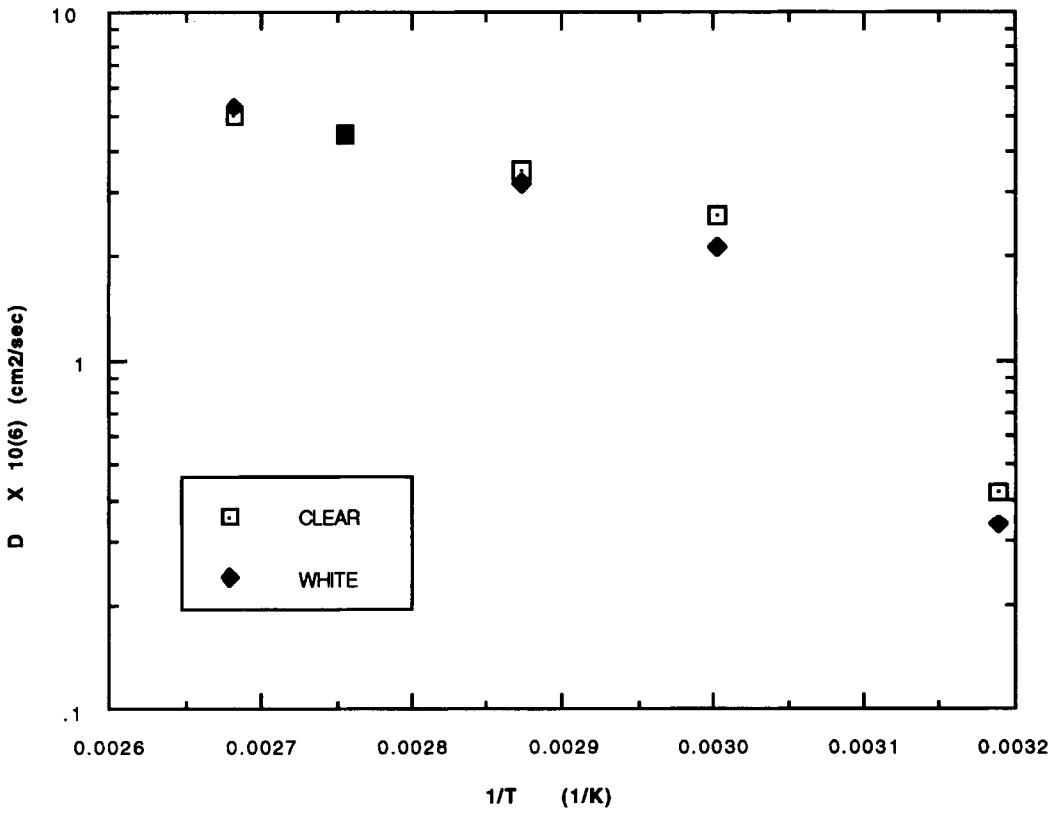

Figure 7 Arrhenius-type plot of the diffusion coefficient vs. inverse temperature for clear and white spandex shows a significant temperature dependence of the diffusion coefficient and a crossover between clear and white values at around 80–85°C.

Fickian diffusion to a limiting relaxation or swelling-controlled sorption may be expected for a given penetrant/polymer system if a sufficient range of temperature and penetrant activity is traversed experimentally.

The values of the diffusion coefficients obtained from the half-time plotted in Figure 7 are in the range of $0.5–6 \times 10^{-6}$ cm^2/s, which are intermediate values typical of diffusion of gases in liquids and polymeric solutions. The nonlinear dependence on temperature, the convex downward curve, and the size of the penetrant DMAc molecules are typical of a diffusion mechanism for large penetrants such as DMAc. A similar temperature dependence has been observed in the past for glassy polymers and also for some polyurethanes.[19] The slopes of these lines are related to the amount of energy required to form the transient voids needed for the diffusion process to occur. There is some indication that the activation energy for diffusion in elastomers approaches a limiting value corresponding to the activation energy for self-diffusion or viscous flow of rubbers.[20] Similar responses have been observed for benzene in poly(ethyl acrylate)[21] and other organic vapor–polymer systems above the glass transition temperature. The physical explanation presented above applies to transport processes in rubbery polymers such as polyethylene, in which penetrants have mobilities governed by the local concentration of sorbate or penetrant. Although the data shown in Figure 7 cannot be represented by an Arrhenius relation with a constant activation energy over the entire range of temperatures, an estimate of the activation energy was calculated for the initial and final slopes to obtain a range of energies over the temperatures studied. These energy values are shown later in Table I.

The same trend in diffusion coefficients is obtained for both clear and white spandex types. The graph in Figure 7 shows a crossover in diffusion coefficients between the clear and white types at about 80–85°C. At lower temperatures, the diffusion coefficient for the clear spandex is higher than that for the white solution. At temperatures below the soft-

Table I Diffusion Coefficients and Activation Energies for Clear Spandex from Sorption Cell Measurements

T (°C)	D_{AV} (cm^2/s) Clear	Activation Energy (cal/g mol)
40	0.416×10^{-6}	3,400 (low T)
60	2.57×10^{-6}	
75	3.50×10^{-6}	
90	4.40×10^{-6}	16,000 (high T)
100	4.97×10^{-6}	

ening transition temperatures of the hard domains, diffusion presumably occurs primarily through the polyether segments of the block polyurethane and the hard domains restrict the mobility of the soft segment. The effect of the additives is not felt until the temperature of the solution is low enough to allow the additives to enhance the aggregation process and thereby increase the desorption rate. The values obtained for the diffusion coefficients are tabulated in Table II. The errors associated with the values are the probable errors calculated from three or more independent runs.[22]

The diffusion coefficients from the sorption cell were compared to data obtained from a stainless-steel devolatilization block[1] and plotted as a function of inverse temperature to compare the activation energies obtained by both methods in Figure 8. It is obvious from these values that not only are the diffusion coefficients an order of magnitude different but also the activation energies are significantly larger for the diffusion obtained in the block. The search for an explanation of the disparity in results was focused on the rate of desorption in the cell. The boundary layer effect should be smaller for desorption into a vacuum, so an alternate explanation for the depressed desorption in the cell was needed. This realization turned attention to the possibility of thermal effects such as those noted by Armstrong and Stannett[10,11] and Hayes and Park.[23,24] Waksman and Schneider[12] measured the diffusion coefficient of toluene in natural rubber by the half-time method or the Joshi–Astarita analysis of coupled diffusion and relaxation and also found that the values leveled off rather than extrapolating to the self-diffusion coefficient of toluene. Application of the Armstrong and Stannett[10,11] treatment of heating effects during sorption led to significant corrections in the diffusion coefficient and to much better agreement with an empirical extrapolation to the self-diffusion coefficient. In applying the analysis to the spandex data for eq. (9), the following values were used: latent heat of vaporization of DMAc, $L = 118$ cal/g; heat capacity, $C_p = 0.5$ cal/g °C; density of the polymer, $\rho = 0.95$ g/cm^3; and the half-thickness, $b = 1.25 \times 10^{-2}$ cm. The heat-transfer coefficients calculated by Armstrong and Stannett from radiation theory and compared to values that they obtained from an unsteady-state heating experiment were in excellent agreement. Their calculations estimated the largest temperature rise during an adsorption experiment to be 1.5°C. The model was applied to incremental measurements of sorption; hence, there was a low change in temperature.

In our work, however, desorption was measured from saturation to vacuum in one step, so it was necessary to physically measure the actual temperature drop that occurred during desorption in order to obtain a reliable value of the heat-transfer coefficient. Foil thermocouples were hung in the sorption cell with spandex dope on them. This feature allowed for measurement of the internal temperature of the polymer dope rather than the surface or surrounding temperatures. These thermocouples are 0.5 mil thick

Table II Diffusion Coefficients for Clear and White Spandex Obtained from Sorption Cell Measurements

Temperature (°C)	Diffusion Coefficient, D_{AV} (cm^2/s) (Clear)	Diffusion Coefficient, D_{AV} (cm^2/s) (White)
40	$0.416 \pm 0.04 \times 10^{-6}$	$0.339 \pm 0.05 \times 10^{-6}$
60	$2.57 \pm 0.04 \times 10^{-6}$	$2.12 \pm 0.04 \times 10^{-6}$
75	$3.50 \pm 0.03 \times 10^{-6}$	$3.22 \pm 0.02 \times 10^{-6}$
90	$4.40 \pm 0.02 \times 10^{-6}$	$4.41 \pm 0.03 \times 10^{-6}$
100	$4.97 \pm 0.08 \times 10^{-6}$	$5.34 \pm 0.04 \times 10^{-6}$

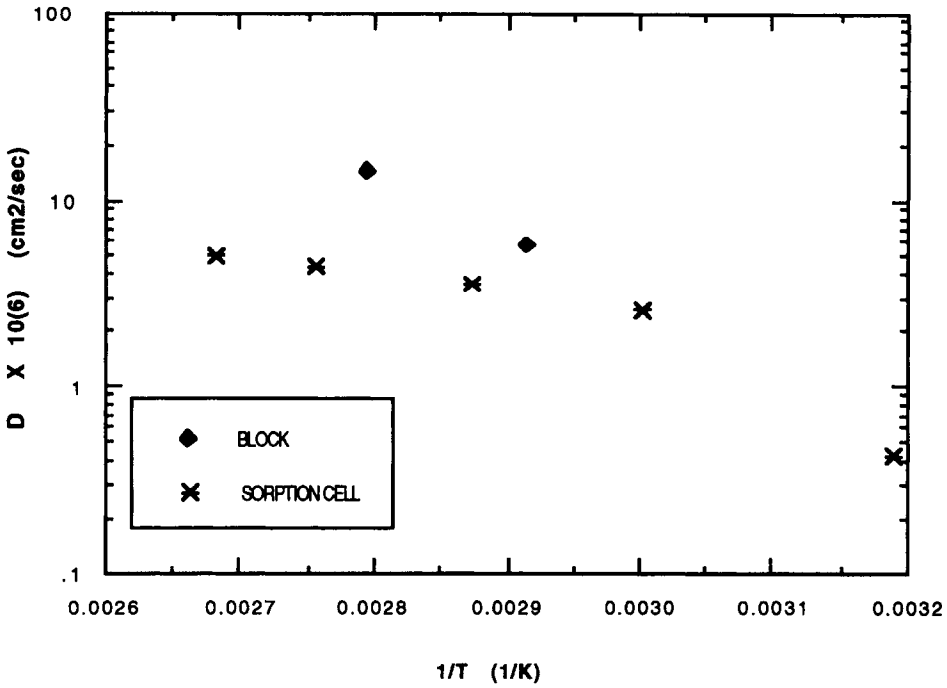

Figure 8 Arrhenius-type plot of diffusion coefficients vs. inverse temperature for clear spandex obtained from the sorption cell compared to those obtained from the stainless-steel devolatilization block.

and have a response time of 0.1 ms. The temperature changes for clear and white spandex were measured at each of the run temperatures. The drop in temperature was from 7 to 30°C for the runs at 40–100°C, respectively, and are tabulated in Table III. The graphs of the temperature drop vs. time are included in the Appendix as Figure A.2 and reflect almost instantaneous drops to the minimum temperature followed by slow recoveries to the temperature of the surroundings.

The heat-transfer coefficients calculated from radiation theory as shown in eq. (10) were calculated with T_0 being the temperature of the surroundings, and T_{inc}, the temperature drop as shown in Table III. The values obtained for the heat-transfer coefficients were on the order of 10^{-4} cal/cm^2 s °C and are tabulated in Table IV. To investigate the sensitivity of the diffusion correction factors to the heat-transfer coefficient, H, two significantly different temperature values were used to estimate H in eq. (10). The first temperature corresponded to the largest excursion from the initial equilibrium temperature, whereas the second corresponded to the temperature at the time when $M_t/M_\infty = 0.5$. These temperatures differ by an order of magnitude, yet the percent correction on **D** differed by less than

Table III Temperature Drops for Clear and White Spandex upon Desorption into Vacuum in the Sorption Cell

Run Temperature (°C)	ΔT (°C) Clear	ΔT (°C) White
40	7	7.5
60	7.3	7.5
75	8	8
90	15	14
100	30	28

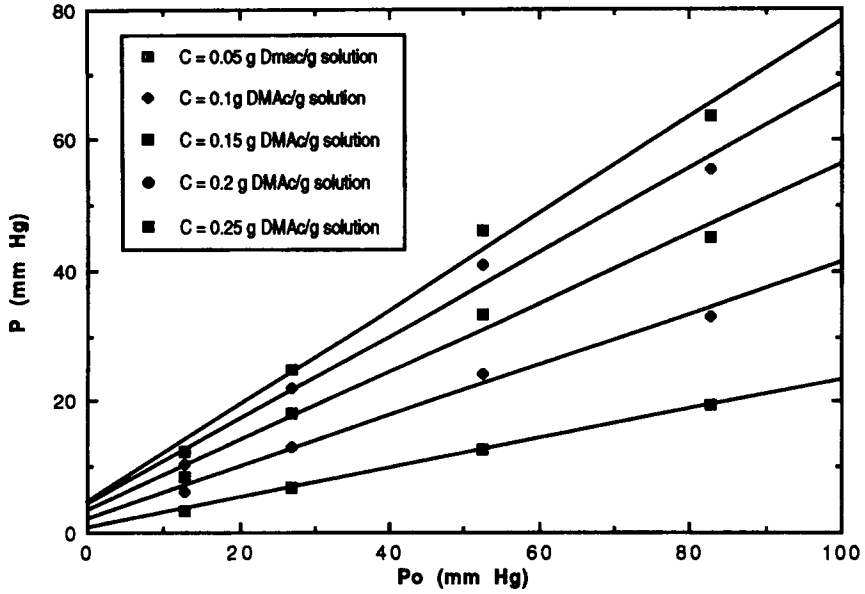

Isostere lines of partial pressure versus vapor pressure obtained from equilibrium sorption measurements.

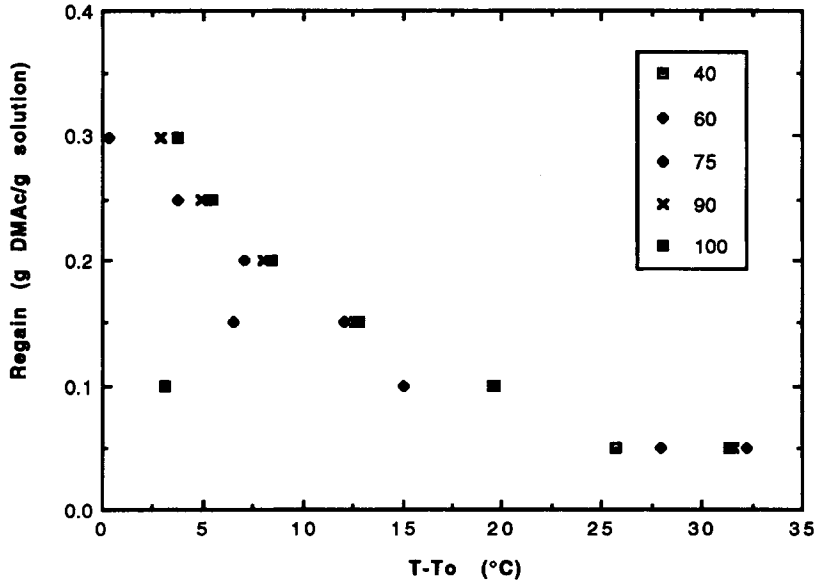

Graph of regain versus temperature difference as obtained from the isostere lines above.

Figure 9 Plots for calculating the temperature coefficient of regain necessary for heat-effect corrections.

10% because the correction is weakly dependent on the estimated value of H used.

There is an implied assumption in the derivation of the model that the temperature within the sample is uniform. This assumption is valid for the case of spandex because of its relatively high thermal conductivity vs. its mass diffusivity and, especially, the large ratio of the thermal conductivity to the heat-transfer coefficient.

The isostere and equilibrium regain vs. temperature plots for the clear samples are shown in Figure 9. These plots correspond to the explanation given for Figure 1(A) and (B). The isosteric heat of sorption was obtained from the slopes of the lines in

Table IV Values of Heat-transfer Coefficients as a Function of Temperature Drop in the Sample for Clear (C) and White (W) Samples

T_0 (°C)	H (C) (cal/cm^2 s K)	H(W) (cal/cm^2 s K)
40	1.609×10^{-4}	1.603×10^{-4}
60	1.942×10^{-4}	1.936×10^{-4}
75	2.219×10^{-4}	2.207×10^{-4}
90	2.439×10^{-4}	2.446×10^{-4}
100	2.494×10^{-4}	2.516×10^{-4}

Figure 9(A). The specific intercept for each concentration has a complex meaning that is not important for the current analysis. The temperature coefficient of regain, ω, calculated from the sorption isotherm data, ranged from 0.00385 to 0.0241 for temperatures from 40 to 100°C, respectively. The % correction for these samples was then obtained using the theoretical calculations shown in Figures 2 and 3.

The values of the diffusion coefficient measured directly from the cell, "Observed diffusion coefficients," and those obtained from the heat-effect calculations, "Corrected diffusion coefficients," are tabulated in Table V along with the percent correction for clear spandex. Similar results were obtained for the white samples as shown in Table VI. The correction factors increased with increasing temperatures and rapidly became several hundred percent.

Figure 10 shows an Arrhenius-type plot of both the observed and corrected diffusion coefficients as well as the diffusion coefficients from the block devolatilization. The slope of the line after correction is still concave, i.e., the diffusion coefficient is still a function of temperature, but not as strongly dependent as it was before the correction was applied. The activation energies obtained from the slopes of the corrected cell values in the lower and upper regions of the graph are in the range of 11,000 to 23,600 cal/g mol, respectively. Similar activation energies were tabulated by Barrer[25] for several penetrant gases in both glassy and rubbery polymers. The data from the semi-infinite slab analysis based on isothermal convective flow of nitrogen over the surface of a pool of the polymer are also shown on the same plot and are now of the same order of magnitude as the corrected values[1]. This agreement tends to verify our belief that the effect of cooling upon desorption plays an important role in the desorption rate from the McBain cell. The diffusion coefficients resulting from the block measurements appear to be a bit lower, possibly due to some cooling effects that are not as strong as in the McBain cell, since the sample is in direct contact with the metal block and liquid mercury. Since the thermal conductivity of the material is large, as the sample loses heat it is replaced by energy from the hot metal faster than it could be through air or vacuum as is the case in the cell.

SUMMARY

Kinetics of desorption have been measured via a traditional McBain spring balance system. Diffusion coefficients were obtained for both clear and white spandex for the range of temperatures between 40 and 100°C. It was observed that the diffusion coefficients for the white sample were larger than those of the clear sample at higher temperatures. Below approximately 80°C, the diffusion coefficient for the white sample was larger, but as the temperature was increased, so did the mobility of the polymer chains, allowing the aggregation kinetics of the white spandex, once nucleated, to take place more rapidly, thereby desorbing faster.

Table V Observed Diffusion Coefficients for Clear Spandex from Cell Measurements vs. the Corrected Values for These from the Heat Analysis and the Percent Correction Obtained

Temperature (°C)	Observed Diffusion Coefficient (cm^2/s)	Corrected Diffusion Coefficients (cm^2/s)	% Correction
40	0.416×10^{-6}	0.506×10^{-6}	21.6
60	2.57×10^{-6}	6.30×10^{-6}	145
75	3.50×10^{-6}	1.86×10^{-5}	432
90	4.40×10^{-6}	3.26×10^{-5}	642
100	4.97×10^{-6}	5.67×10^{-5}	1042

Table VI Observed Diffusion Coefficients for White Spandex from Cell Measurements vs. the Corrected Values for These from the Heat Analysis and the Percent Correction Obtained

Temperature (°C)	Observed Diffusion Coefficient (cm^2/s)	Corrected Diffusion Coefficients (cm^2/s)	% Correction
40	0.339×10^{-6}	0.417×10^{-6}	23.4
60	2.12×10^{-6}	5.34×10^{-6}	152
75	3.22×10^{-6}	1.72×10^{-5}	433
90	4.41×10^{-6}	3.25×10^{-5}	638
100	5.34×10^{-6}	5.98×10^{-5}	1020

A comparison was made to diffusion coefficients measured with the aid of a devolatilization block simulating semi-infinite slab conditions.[1] Diffusion coefficients obtained via this block method were an order of magnitude larger than those observed in the cell measurements.

The discrepancy in values of diffusion coefficients for spandex from the two different methods was found to be due to heat effects during the desorption process. Measurements of the temperature of the sample during desorption showed drops in temperature of up to 30°C during desorption when the sample and the surroundings were preheated to 100°C. Heat effects were found to be important, unlike in most cases where the heat of vaporization of the solvents used is low. Application of a model derived to account for the effects of cooling during desorption or heating during sorption to the data obtained from the cell measurements revealed correction factors on the order of several hundred per-

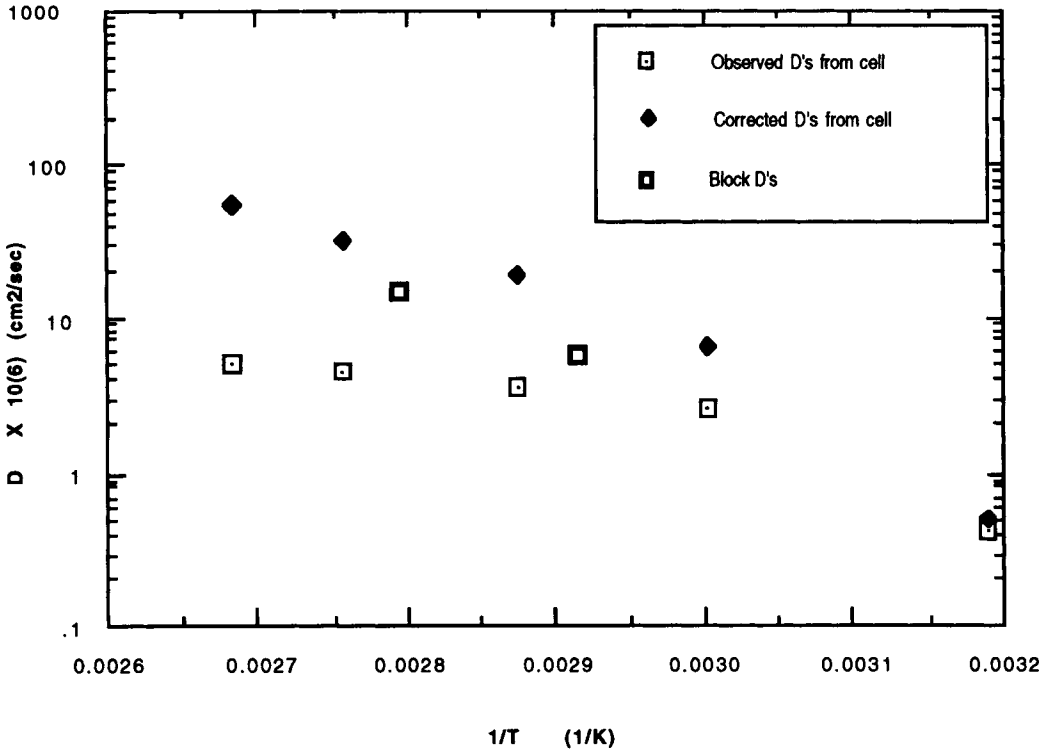

Figure 10 Overall comparison of all diffusion coefficients for clear spandex; the block results are now comparable to the corrected values as shown in Figure 8 instead of being an order of magnitude away from the observed results in the sorption cell.

cents. All diffusion coefficients, after corrections, were of the same order of magnitude, and the block diffusion coefficients were slightly lower since they were not corrected for possible heat effects. Being in direct contact with metal allowed the sample in the block to transfer lost heat back into the solution faster, thus not being as strongly affected by this effect.

APPENDIX: DERIVATION OF HEAT TRANSFER COEFFICIENT EQUATION

From the definition of heat-transfer coefficients, H (Ref. 13, p. 391),

$$Q = HA\Delta T = HA(T_0 - T_{inc}) \qquad (A.1)$$

where Q is the heat flow into the fluid; A, a characteristic area, and ΔT, a characteristic temperature difference; the heat-transfer coefficient is the proportionality factor in the relation. This amount of heat transferred into the body can be equated to the heat radiated into black bodies in a vacuum by Lambert's law (Ref. 13, p. 437):

$$Q_{12} = AF\sigma(T_1^4 - T_2^4) \qquad (A.2)$$

where Q_{12} is the net energy transferred from an isothermal black body "1" to another isothermal black body "2"; F, the view factor that can be set equal to 1; A, the area of body "2"; and σ, the Stefan–Boltzmann constant, $\sigma = 1.355 \times 10^{-12}$ cal/s cm^2 K^{-4}. By setting body "1" to be the surroundings or system temperature and body "2" as the sample temperature, we can express eq. (A.2) as

$$Q = A\sigma(T_0^4 - T_{inc}^4) \qquad (A.3)$$

and equate it to eq. (A.1) to obtain

$$Q = A\sigma(T_0^4 - T_{inc}^4) = HA(T_0 - T_{inc}) \qquad (A.4)$$

which upon canceling of the areas can be expanded as

$$\sigma(T_0^2 + T_{inc}^2)(T_0 - T_{inc})(T_0 + T_{inc}) = H(T_0 - T_{inc}) \qquad (A.5)$$

and reduced to solve for the heat-transfer coefficient as

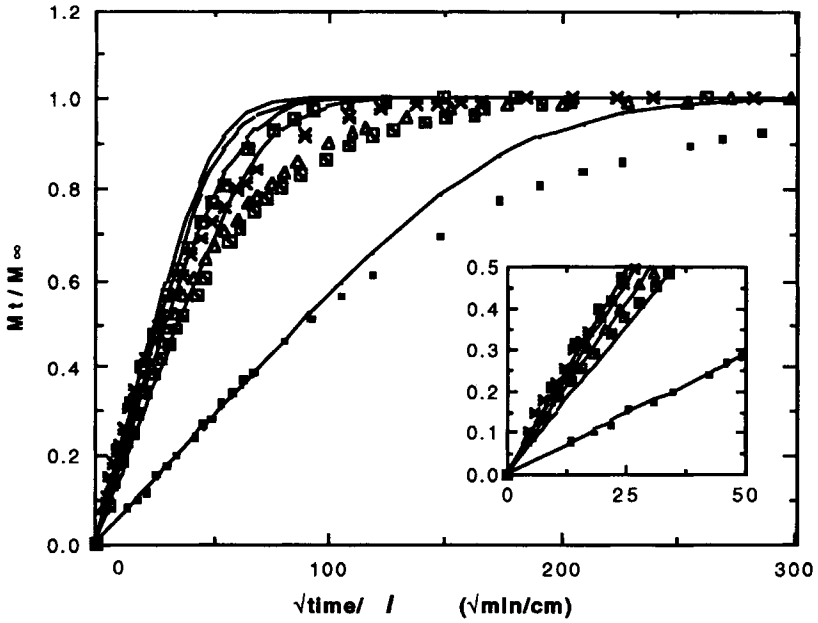

Figure A.1 Graph of theoretical Fickian curves obtained from the short- and long-term response equations based on the diffusion coefficients calculated from the cell measurements vs. the data from those runs for clear spandex.

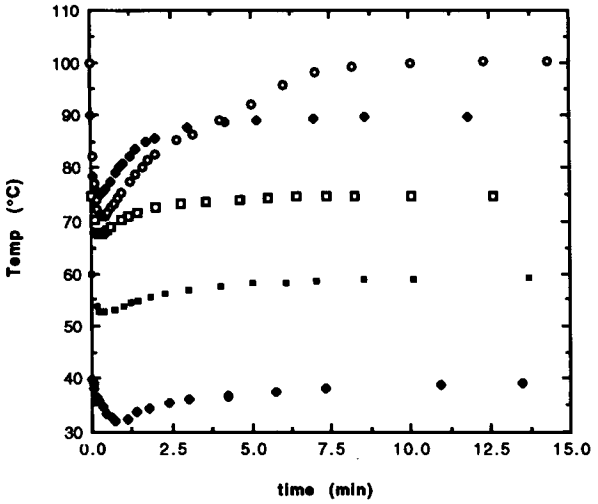

Figure A.2 Temperature of the sample upon desorption for runs of 40–100°C vs. time. Temperatures shown are for clear spandex; similar results were obtained for white spandex as summarized in the text.

shown by eq. (21) in the text:

$$H = \sigma(T_0 + T_{inc})(T_0^2 + T_{inc}^2) \qquad (A.6)$$

REFERENCES

1. M. M. Gou, M. S. Thesis, *"Sorption/Desorption Processes for DMAc in Spandex."*
2. W. Steuber, U.S. Pat. 2,929,804 (March 22, 1960).
3. M. M. Gou, W. J. Koros, and G. W. Goldman, *J. Appl. Polym. Sci.*, **43,** 1991 (1991).
4. J. Crank, *The Mathematics of Diffusion,* 2nd ed., Clarendon Press, Oxford, 1975.
5. J. Crank and G. S. Park, *Trans. Faraday Soc.*, **45,** 240 (1949).
6. H. Fujita, *Fortschr. Hochpolym.-Forsch.* **3** (1961).
7. J. Crank and G. S. Park, *Diffusion in Polymers,* Academic Press, London, 1968.
8. H. Odani, M. Uchikura, K. Taira, and M. Kurata, *J. Macromol. Sci.-Phys. B,* **17**(2), 337 (1980).
9. K. T. Chiang, and M. V. Sefton, *J. Polym. Sci. Phys. Ed.*, **15,** 1927 (1977).
10. A. A. Armstrong, Jr. and V. Stannett, *Makromol. Chem.*, **90,** 145 (1966).
11. A. A. Armstrong, Jr., J. D. Wellons, and V. Stannett, *Makromol. Chem.*, **95,** 78 (1966).
12. L. S. Waksman, N. S. Schneider, and N.-H. Sung, in *Barrier Polymers and Barrier Structures,* W. J. Koros, Ed., American Chemical Society, Washington DC, 1990, Chap. 20.
13. R. B. Bird, W. E. Stewart, and E. N. Lightfoot, *Transport Phenomena,* Wiley, New York, 1960.
14. DMAc (Dimethylacetamide) Product Information, Chemical Properties, Table 1, ETL, E. I. DuPont de Nemours, Wilmington, DE 19880.
15. R. McGregor, *Diffusion in Fibers and Films,* Academic Press, New York, 1974.
16. H. L. Frisch, *J. Polym. Sci. B,* **3,** 13 (1965).
17. A. R. Berens and H. B. Hopfenberg, *Polymer,* **19,** 489 (1978).
18. H. B. Hopfenberg and H. L. Frisch, *J. Polym. Sci. B,* **7,** 405 (1969).
19. J. S. McBride, T. A. Massaro, and S. L. Cooper, *J. Appl. Polym. Sci.*, **23,** 201 (1979).
20. G. J. Van Amerongen, *Rubber Chem. Technol.*, **37,** 1065 (1964).
21. W. J. Koros and H. B. Hopfenberg, *Food Technol.*, **April,** 56–60 (1979).
22. Y. Beers, *Introduction to the Theory of Error,* Addison-Wesley, Reading, MA, 1962.
23. M. J. Hayes and G. S. Park, *Trans. Faraday Soc.*, **51,** 1134 (1955).
24. M. J. Hayes and G. S. Park, *Trans Faraday Soc.*, **52,** 949 (1956).
25. R. M. Barrer, *J. Phys. Chem.*, **61,** 178 (1957).

Received October 16, 1992
Accepted July 17, 1993